Co-precipitation of oppositely charged nanoparticles: the case of mixed ligand nanoparticles

2015 J. Phys. D: Appl. Phys. 48 434001

(http://iopscience.iop.org/0022-3727/48/43/434001)

IOP Publishing Journal of Physics D: Applied Physics
J. Phys. D: Appl. Phys. **48** (2015) 434001 (7pp) doi:10.1088/0022-3727/48/43/434001

Co-precipitation of oppositely charged nanoparticles: the case of mixed ligand nanoparticles

Mauro Moglianetti[1,2,6] Evgeniy Ponomarev[2,3,6] Maxime Szybowski[2], Francesco Stellacci[2] and Javier Reguera[2,3,5]

[1] Center for Biomolecular Nanotechnologies (CBN), Istituto Italiano di Tecnologia, 73010 Arnesano, Italy
[2] Institut des Matériaux, École Polytechnique Fédérale de Lausanne, 1015 Lausanne, Switzerland
[3] Deparment of Physics, University of Geneva, 1205 Geneva, Switzerland
[4] CIC BiomaGUNE, Paseo de Miramón 182C, 20009 Donostia-San Sebastián, Spain
[5] Ikerbasque, Basque Foundation for Science, 48011 Bilbao, Spain

E-mail: jreguera@cicbiomagune.es and francesco.stellacci@epfl.ch

Received 13 May 2015, revised 21 July 2015
Accepted for publication 7 August 2015
Published 29 September 2015

Abstract

Colloid stability is of high importance in a multitude of fields ranging from food science to biotechnology. There is strong interest in studying the stability of small particles (of a size of a few nanometres) with complex surface structures, that make them resemble the complexity of proteins and other natural biomolecules, in the presence of oppositely charged nanoparticles. While for nanoparticles with homogeneously charged surfaces an abrupt precipitation has been observed at the neutrality of charges, data are missing about the stability of nanoparticles when they have more complex surface structures, like the presence of hydrophobic patches. To study the role of these hydrophobic patches in the stability of nanoparticles a series of negatively charged nanoparticles has been synthesized with different ratios of hydrophobic content and with control on the structural distribution of the hydrophobic moiety, and then titrated with positively charged nanoparticles. For nanoparticles with patchy nanodomains, the influence of hydrophobic content was observed together with the influence of the size of the nanoparticles. By contrast, for nanoparticles with a uniform distribution of hydrophobic ligands, size changes and hydrophobic content did not play any role in co-precipitation behaviour. A comparison of these two sets of nanoparticles suggests that nanodomains present at the surfaces of nanoparticles are playing an important role in stability against co-precipitation.

Keywords: colloidal stability, charged nanoparticles, patchy nanoparticles, co-precipitation

(Some figures may appear in colour only in the online journal)

1. Introduction

The study of colloids has strong implications in many aspects of our daily life, from paints and inks to biological fluids and food. In food, colloids are present almost everywhere, in products ranging from milk and wine to a plethora of preparations in modern cuisine such as emulsions, foams, creams, etc [1]. The characteristics of a specific kind of food not only depend on its organoleptic properties but also on the colloid's characteristics such as the size of the dispersed phase or the colloidal stability. Apart from daily-life products, the study of colloids has strong implications in many technological fields such as electronics [2], photonics [3], medicine [4], analytics [5], and almost all nanotechnological fields [6]. The stability of

[6] These authors contributed equally to this work.

colloids is perhaps the most important property as it depends on how particles interact with one another and how they form agglomerates or aggregates or how they coalesce on bigger particles. Derjaguin, Landau, Verwey and Overbeek (DLVO) created in the middle of the last century a formalism that explains the aggregation of aqueous dispersions as the balance between Van der Waals and electrostatic forces [7]. Since then, new improvements have appeared that include additional forces or that better describe how ions in solution interact with the surface of the particles changing their stability [8].

A promising method to study the properties of nanometre-sized colloids is one based on the study of the interaction between particles of opposite charges. This interaction highly depends on the size regime of the dispersed particles. Oppositely charged complexing ions are stable in solutions until they reach a certain entire number n in the ratio $[A^-]/[C+]$, where $[A^-]$ is the anion and $[C^+]$ is the cation concentration. By contrast, oppositely charged microparticles precipitate continuously due to the high Van der Waals interactions and poor solvation of large aggregates. When particles are in the nanometric regime, their aggregation, and hence precipitation, happens at the neutrality of charges like some ionic salts, i.e. $[A^-]/[C+] = 1$ [9–12]. It hasn't been until recently that the mechanism of precipitation of mixtures of oppositely charged colloids with diameter sizes going from a few to tens of nanometres has been elucidated. This process is explained as a balance between several factors, first and most importantly, the high surface-to-volume ratio of nanoparticles that allows an extremely high concentration of charges in low volumes (this kind of nanoparticles is also called 'nano-ions'). This high concentration of charges allows therefore a high electrostatic and a low Van der Waals interaction. Secondly, the geometry of the nanoparticle system plays an important role as it allows having several particles of one charge surrounding a nanoparticle of the opposite charge while maintaining the distance between nanoparticles of the same charge to be high enough to decrease nanoparticle repulsion thanks to the shielding effect of the counter ions in solution. The equal size of spherical oppositely charged nanoparticles in co-precipitation and the repulsion between nanoparticles of the same charge cause the formation of suprastructures that are not common for spherical nanoparticles like the case of a diamond-like crystalline suprastructure [10, 13]. Apart from spherical nanoparticles, the co-precipitation of oppositely charged nanoparticles has also been observed for nanorods [14] and for spherical nanoparticles with different polydispersities [10]. Most of these studies have mainly focused on metallic nanoparticles covered by 11-mercaptoundecanoic acid (MUA) for the case of negatively charged nanoparticles, and *N*,*N*,*N*- trimethyl(11-mercaptoundecyl)ammonium (TMA) for the case of positive charges. Very little is known about the co-precipitation behaviour of nanoparticles with differently charged ligands and of nanoparticles covered by a mixture of ligand molecules. To the best of our knowledge there is only one experiment on nanoparticles covered by a mixture of different ligands in which a mixture of MUA and the hydrophilic ligand 11-mercaptoundecanol (MUO) was covering the surface of the nanoparticles [11]. The co-precipitation behaviour of these nanoparticles showed the expected result of precipitation at the composition where the charges on both particles were of the same number. Data are missing on the co-precipitation behaviour of charged nanoparticles covered by a mixture of ligands that form nanostructure-like patches (hydrophilic–hydrophobic) on the surfaces of the nanoparticles.

Self-assembled monolayers composed of two dislike thiolated molecules on the surface of metallic nanoparticles tend to arrange in small narrow nanodomains, also called patches or stripes, around 1 nm in thickness [15, 16]. Different techniques have shown their existence, including high-resolution scanning tunnelling microscopy (STM) [17], NMR [18], mass spectrometry [19] and neutron scattering [20]. The formation of narrow nanodomains is believed to be due to an entropic contribution arising from the mixing of ligand molecules of different lengths and bulkiness at the nanoparticle surfaces. When long ligands are surrounded by short ones, there is an increase in the available space of the long ligands, and hence, an increase in entropy that overcomes the enthalpic effect of approaching ligands of different nature [21]. The presence of small hydrophobic domains can change the way in which these nanoparticles interact with their environment as it is in the case of proteins characterized by the presence of nanodomains. Nanoparticles covered with charged moieties of sulfonic acid and hydrophobic nanodomains have shown, for example, a cell-membrane-penetrating behaviour, crossing the membrane like cell-penetrating peptides [22]. On the other hand this penetration is inhibited when the hydrophobic ligands are subsisted by bulkier molecules that inhibit the formation of nanodomains giving rise to a random distribution of ligands [22]. It has also been observed that the nanodomain formation changes the interfacial energy between the nanoparticles and the surrounding solvent. Kuna *et al* [23] showed that with nanoparticles covered by two ligands, one hydrophobic and one non-charged hydrophilic, the interfacial energy not only depends on the chemical composition but there is also a structural component of the interfacial energy that can be up to 30% of the total interfacial energy. This extra component in the interfacial energy is produced by the presence of small domains that are commensurate with a few water molecules. This leads to two opposite effects: water molecules that are trapped in hydrophilic domains decrease their entropy due to the reduced space and make solvation less favourable (confinement effect) [24], whilst the decrease in water density close to the hydrophobic surface is affected by the lateral hydrophilic domains and it has the effect of increasing solvation and decreasing the interfacial energy (cavitation effect). Changing the ratio between the two ligands on the nanoparticles produces a change in the domain size and shape producing a non-monotonic behaviour of the change of interfacial energy with the ligand ratio of the nanoparticles.

In this work, we have tried to investigate the contribution of nanoparticles' hydrophobic nanodomains in the interaction with oppositely charged nanoparticles and, hence, the stability of the colloidal solution by comparing two different systems. In co-precipitation several simultaneous effects are expected, including the decrease of charges due to the substitution of charged ligands by hydrophobic ligands and therefore the

decrease of Coulombic attraction, the decrease of stability due to the increase of hydrophobicity, and the effect of nanodomains on the surface of the nanoparticles that changes the way the nanoparticle surfaces are hydrated. As a way to characterize the influence of the nanodomains, two sets of gold nanoparticles were synthesized. The first set is composed of negatively charged gold nanoparticles with hydrophobic nanodomains, synthesized using MUA and 1-octanethiol (OT) as charged and hydrophobic ligands respectively at different ratio compositions. These nanoparticles have shown narrow nanodomains on STM experiments with a low percentage of Janus nanoparticles [25]. The second set is composed of gold nanoparticles covered with negatively charged and hydrophobic ligands, synthesized with MUA and 3,7-dimethyloctane-1-thiol (branched OT or brOT) ligands. The brOT ligands, as it has been shown earlier, should inhibit the crystallization and nanodomain formation on the surface of the nanoparticles, giving rise to a random distribution of ligands [22]. Changing the ratio of MUA : OT ligands would produce changes in the nanodomain areas on the nanoparticle surface. Changes in the ligand arrangements could alternatively be obtained by changing the length mismatch of the ligands. However, there are no STM data about nanodomain characteristics for other length mismatches.

Titrations were performed with the addition of aliquots of a solution of TMA nanoparticles to a solution of MUA : OT and MUA : brOT nanoparticles at different ligand ratios and the experiment was monitored by UV–vis spectrometry. The different sets of nanoparticles were characterized by transmission electron microscopy (TEM), thermogravimetric analysis (TGA) and ^{1}H nuclear magnetic resonance (NMR). From those results the ratio of positive charges over the total charges at which co-precipitation took place was represented as a function of the hydrophobic ligand ratio present on the nanoparticles. Additionally pH titration experiments were performed on the mixed-ligand nanoparticles to guarantee the fully charged state of the nanoparticles during the co-precipitation experiments. These measurements also allowed the evaluation of the influence on the pKa of the hydrophobic nanodomains in the proximity of carboxylic acids as well as the increase of the separation between carboxyl species.

2. Experimental

2.1. Materials

N,*N*,*N*-trimethyl(11-mercaptoundecyl)ammonium chloride was purchased at Prochima Surfaces Sp. (Poland). 1-Octanethiol, 11-mercaptoundecanoic acid and the rest of the reagents were provided by Sigma-Aldrich. 3,7-Dimethyloctane-1-thiol was synthesized as described previously [22].

2.2. Synthesis of nanoparticles

Gold nanoparticles covered by different alkane thiols were synthesized using a modification of the method described by Zheng *et al* [26, 27]. Basically, 0.25 mmol chloro(triphenylphosphine) gold was dissolved in 20 ml of toluene : methanol 1 : 1 (v/v) and 0.25 mmol of ligands at different ligand ratios were added and mixed for 10 min. After that 2.5 mmol of a morpholine–borane complex dissolved in 20 ml of toluene : methanol 1 : 1 (v/v) was added to reduce the gold salt. Once added, the solution was put immediately to reflux at 95 °C and left to react for one hour under strong stirring. The sample was precipitated with toluene and purification was made in at least five cycles of centrifugation with acetone. The nanoparticles were dried under vacuum for at least 24 h.

Table1. Characterization parameters of the nanoparticles.

Nanoparticle	Ξ ((br)OT)[a]	Au/ligand (m/m)[b]	Diameter (nm)[c]
TMA	—	6.1	4.5 ± 0.8
MUA	—	6.8	4.1 ± 0.8
MUA : OT			
	0.09	6.9	4.6 ± 0.5
	0.17	7.2	4.7 ± 0.7
	0.22	7.5	4.7 ± 0.8
	0.27	7.5	4.6 ± 0.7
	0.30	7.3	4.4 ± 0.8
	0.34	8.3	4.8 ± 0.7
	0.35	7.3	4.6 ± 0.8
MUA : brOT			
	0.06	7.6	4.9 ± 0.6
	0.70	7.8	5.1 ± 0.6
	0.11	7.9	5.8 ± 0.7
	0.12	7.8	5.2 ± 0.6
	0.19	8.6	5.8 ± 0.6
	0.23	8.7	5.8 ± 0.7
	0.30	10.8	5.9 ± 0.7
	0.33	11.2	5.8 ± 0.7

[a] Molar fraction of the ligand OT or brOT with respect to the total quantity of ligands measured by NMR.
[b] Ratio in mass between the inorganic and the organic part of the nanoparticles measured by TGA.
[c] Average diameter and standard deviation measured by TEM.

2.3. Nanoparticle characterization

TEM: TEM images were taken in a Philips/FEI CM12 operating at 120 kV and analysed by ImageJ software [28]. Between 1000 and 3000 nanoparticles from at least three images were measured using the standard threshold method. Diameters and standard deviations were obtained assuming spherical geometry. The TEM core sizes are shown in table 1.

TGA: A PerkinElmer TGA400 set-up was used for thermogravimetric analysis. Nanoparticles were placed in a crucible and heated from 35 to 850 °C at 10 °C min^{-1}. Mass ratios between the gold and ligands were established by comparing the initial mass to the final mass corresponding to the nanoparticle cores. The mass ratios are shown in table 1.

NMR: ^{1}H NMR was measured in a Brucker 400. 5 mg of NPs were dissolved in deuterated methanol and etched with KCN overnight and then measured directly on NMR. The ligand ratios were evaluated by comparing the CH_2 group close

to the carboxyl with the CH_3 terminal groups of the aliphatic ligands. The final nanoparticle composition can be observed in table 1 for MUA : OT and MUA : brOT respectively.

UV–VIS: UV–vis spectra were recorded on a QE65000 scientific-grade spectrometer in the range 200–900 nm in an optical cell. A cuvette with a solution with negatively charged nanoparticles was kept under stirring and the spectra were recorded after 5 min of every addition of the solution with oppositely charged nanoparticles at the same concentration.

pH titration: several nanoparticles at different ligand ratios were titrated to evaluate the influence of the ligand ratio on the pKa. The pH titration was performed with a modification of previously described methods [29, 30]. A solution of 5 mg of nanoparticles in 12 ml of water and 240 μl of 50mM tetramethylammonium hydroxide (TMAOH) was prepared and left stirring for 5 min to ensure a good dispersion of the nanoparticles. Then 200 μl of 50mM HCl was added to the solution to start the titration from a higher pH value, and water was added to reach 15 ml. The titration was performed with 5 ml of the mother solution freshly prepared, adding 3 ml of water and 0.8 ml of 1M of tetramethylammonium chloride (TMACl) to fix the ionic strength, and then titrated with 80 μl aliquots of 2mM HCl. From the titration curves obtained, we assessed the apparent pKa using the derivate of the curves. The apparent pKa was defined as the pH at which the derivative reaches a local maximum.

2.4. Titration experiments

An initial solution of positively charged TMA nanoparticles and negatively charged nanoparticles of MUA, MUA–OT and MUA–brOT was prepared at the same concentration (4mM in terms of gold atoms) and then diluted to 0.5 mM to perform the experiment. The concentration was further controlled using UV–vis absorbance versus the concentration calibration curve previously measured. The pH was initially adjusted to ~12 adding a small amount of 0.2M $N(CH_3)_4OH$. Aliquots of TMA nanoparticle solutions were added in a step-wise manner to the titrated solution containing negatively charged nanoparticles. In each step, the mixtures were magnetically stirred for 5 min before measuring the solution with a UV–vis spectrophotometer.

In order to evaluate the titration in terms of the ratio of the charges the χ parameter was calculated from the initial mass of the nanoparticles used to prepare the titration solutions and by using the NMR and TGA measurements of those nanoparticles. The χ parameter is defined as the ratio between the number of positive charges and the overall number of charges at a certain titration step. Assuming that the amount of charges in the core is negligible with respect to the charges coming from the ligands, we can calculate χ as:

$$\chi = \frac{N^+}{N^+ + N^-} = \frac{N_{\text{ligands}}^{\text{TMA}}}{N_{\text{ligands}}^{\text{TMA}} + N_{\text{ligands}}^{\text{MUA}-(\text{br})\text{OT}} \times f^{\text{MUA}}}, \quad (1)$$

where f^{MUA} is the molar fraction of the MUA molecules in the MUA–(br)OT nanoparticles calculated by ^{1}H NMR; $N_{\text{ligands}}^{\text{TMA}}$, $N_{\text{ligands}}^{\text{MUA}-(\text{br})\text{OT}}$ are the number of ligands of TMA and mixed MUA–(br)OT respectively.

The calculation of $N_{\text{ligands}}^{\text{TMA}}$ and $N_{\text{ligands}}^{\text{MUA}-\text{OT}}$ is based on the ligands/gold mass ratio obtained from the thermogravimetric analysis. Therefore the number of ligands for a certain solution concentration is:

$$N_{\text{ligands}}^{\text{MUA}-(\text{br})\text{OT}} = \frac{c^{\text{MUA}-(\text{Br})\text{OT}} \times V^{\text{MUA}-(\text{br})\text{OT}} \times r_{\text{lig/Au}}}{(f^{\text{MUA}} \times \text{MW}_{\text{MUA}} + (1 - f^{\text{MUA}}) \times \text{MW}_{(\text{br})\text{OT}})}, \quad (2)$$

where MW_{MUA} is the molar weight of MUA, and $r_{\text{lig/Au}}$ is the ligands/gold mass ratio.

$$N_{\text{ligands}}^{\text{TMA}} = \frac{c^{\text{TMA}} \times V^{\text{TMA}} \times r_{\text{lig/Au}}}{\text{MW}_{\text{TMA}}}, \quad (3)$$

where MW_{TMA} is the molar weight of TMA.

3. Results and discussion

In this work, we have studied the stability of metallic nanoparticles covered by MUA and OT (linear and branched) in different ratios in an experiment of co-precipitation with oppositely charged nanoparticles. Different thiolated Au nanoparticles were synthesized with different ligand ratios, keeping a relatively low size polydispersity (always below 20%) and diameters ranging between 4 and 6 nm. The precipitation point of the nanoparticles covered by different binary mixtures of ligands induced by the addition of charged nanoparticles covered by TMA was obtained using UV–vis measurements. Figure 1(a) shows an example of the titration experiments—a MUA : OT 4 : 1 nanoparticle solution titrated by TMA nanoparticles. During the initial part of the titration no big changes are reflected either in the spectrum shape or on absorbance at the maximum of the SPR. However after a certain value, the solution rapidly aggregates and precipitates producing a sharp decrease in the solution absorbance (figure 1(b)). We have selected the middle point of the precipitation after a fitting to a sigmoidal shape to characterize the data in a more operator-independent way and the measurements were repeated three times to evaluate the accuracy of the results.

Previous reports showed that oppositely charged nanoparticles precipitate when their charges are compensated and that the precipitation point could be determined with an error below 3% between different experiments [9]. We decided to use co-precipitation to examine the influence of hydrophobic patches on the interfacial properties of these nanoparticles. For that, different titration experiments were performed on nanoparticles covered with negatively charged and hydrophobic ligands at different ratios and therefore different nanodomains in terms of number and probably size. A complete characterization of the nanoparticles using TEM, NMR (before and after etching of the gold core) and TGA was performed allowing us to precisely evaluate the balance of charges required to induce the precipitation of the solution as a function of the amphiphilicity of our nanoparticles. This information plays a crucial role as the amount of hydrophobic ligands determines the charge density on the shell and the nanodomains' characteristics.

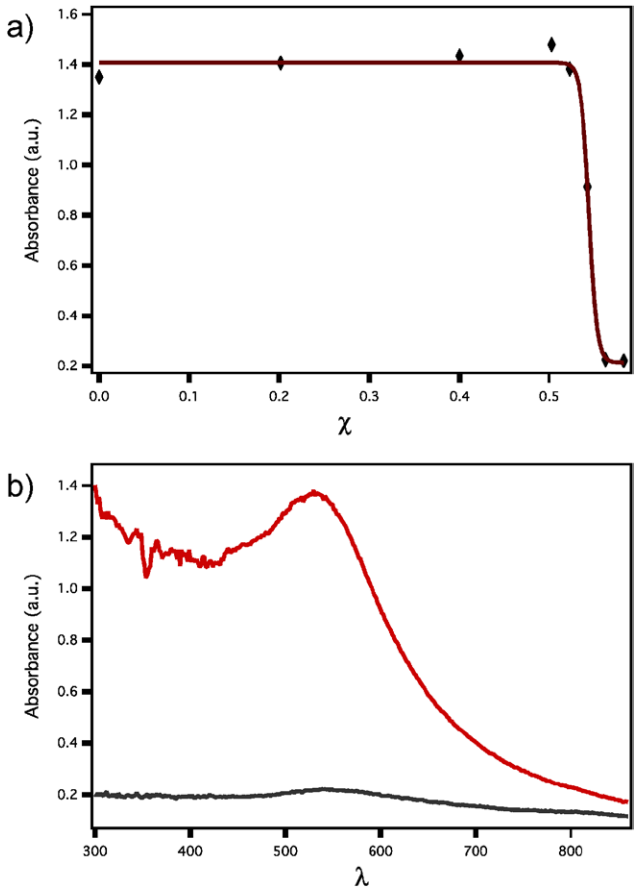

Figure 1. Example of a titration experiment—MUA–OT 4 : 1 nanoparticles titrated with TMA nanoparticles. (a) Absorbance at surface plasmon resonance maximum at different charge ratios, χ. Experimental data (solid diamond) is fitted with sigmoid function (solid line). (b) UV–vis absorbance curves before (red, upper line) and after (black, lower line) the precipitation point.

Figure 2 shows the results obtained from the co-precipitation experiment for MUA : OT and MUA : brOT. The value of χ for the MUA nanoparticles (i.e. for $\Xi(\mathrm{OT}) = 0$) is slightly lower than the one obtained by Kalsin *et al* [9], i.e. it doesn't correspond exactly with the neutrality of charges but it indicates that for homoligand nanoparticles the precipitation point of the titration takes place with a lower addition of positive charges ($\chi \sim 0.45$). This subtle difference could be attributed to the different method used to determine the precipitation point. Furthermore, we adopt a quantification method based on TGA that is different from the one reported by Kalsin *et al* [9] where a fixed density of the ligands was assumed at the surface of the nanoparticles.

For the MUA : OT series the addition of hydrophobic ligands strongly influences the precipitation point with a shift towards higher values. At a 0.1 molar fraction of OT we observe a significant increase of almost 0.1 units of χ. Interestingly for a further increase of the hydrophobic content, no significative increase is observed. The trend doesn't correspond to a linear increase of χ up to a hydrophobic content of 0.3. At 0.35 we observe an abrupt change in χ, followed by a decrease in the following point that causes a non-monotonic behaviour of χ versus $\Xi(\mathrm{OT})$. After this point the experiment cannot be performed anymore as the hydrophobic content makes the nanoparticles insoluble in water.

Size changes between the different MUA : OT series could play a role in the co-precipitation behaviour as the changes in χ could also be related to the changes in sizes of the nanoparticles. However, as shown in figure 2, the differences in nanoparticle size distribution within the MUA : OT series and with the TMA nanoparticles are very small (less than half a nanometre apart). In a previous report Kowalczyk *et al* demonstrated that the co-precipitation of nanoparticles with an overlap of the size distribution of the two nanoparticle systems leads to the formation of diamond-like crystals [31]. The MUA : OT series presented in this work can probably be included in this category as the size distributions of the nanoparticles are less than half a nanometre apart. Further deductions from a comparison with the results presented in reference [31] are difficult as in this last case the aggregates were formed under a slow crystallization process in a DMSO/water mixture instead of a titration procedure.

A strong suggestion on the role of nanodomains in influencing the co-precipitation behaviour of nanoparticles comes from a comparison with the MUA : brOT nanoparticles. The MUA : brOT χ values show a flat trend with similar values to the co-precipitation point of homoligand nanoparticles and only a slight uprising at a 0.3 molar fraction. It is clear that nanoparticle size changes in the case of MUA : brOT don't play a role in varying the co-precipitation point.

A comparison between these two systems (MUA : OT and MUA : brOT) strongly points to a role in the co-precipitation of the nanostructuring present on the interface of the MUA : OT system. As determined in the literature, the branching of hydrophobic ligands strongly disfavours the formation of nanodomains and promotes a random distribution of hydrophobic ligands instead of the formation of patches on the surface. As our data show, the addition of hydrophobic ligands doesn't change the ratio of charges at which precipitation takes place unless they are organized in hydrophobic patches.

Therefore this indicates that the co-precipitation behaviour of MUA : OT is related to the presence of hydrophobic ligands distributed in differently shaped nanodomains. This nanostructuring plays a role in changing the interfacial properties of the nanoparticles. The hydrophobic content on the surface changes the point at which the nanoparticles precipitate. χ represents the amount of charges and not of nanoparticles; therefore the increase in χ for MUA : OT suggests that it is necessary to introduce more positive charges to precipitate the system. A further increase of the hydrophobic content up to a 0.3 OT fraction does not change χ. The last change at high values of hydrophobic content could be related to an increase in the instability of the nanoparticles as we approach the unstable ratio at which the nanoparticles are insoluble.

Another important player in the co-precipitation experiment is the pH at which the experiment is performed. In order to calculate the ratio of charges from the ligand concentration measured by TGA and NMR, MUA ligands should all be in a charged state. The carboxyl group of MUA can have two different states, as carboxyl at low pH or as carboxylate (negatively charged) at high pH. To ensure that the titrations were

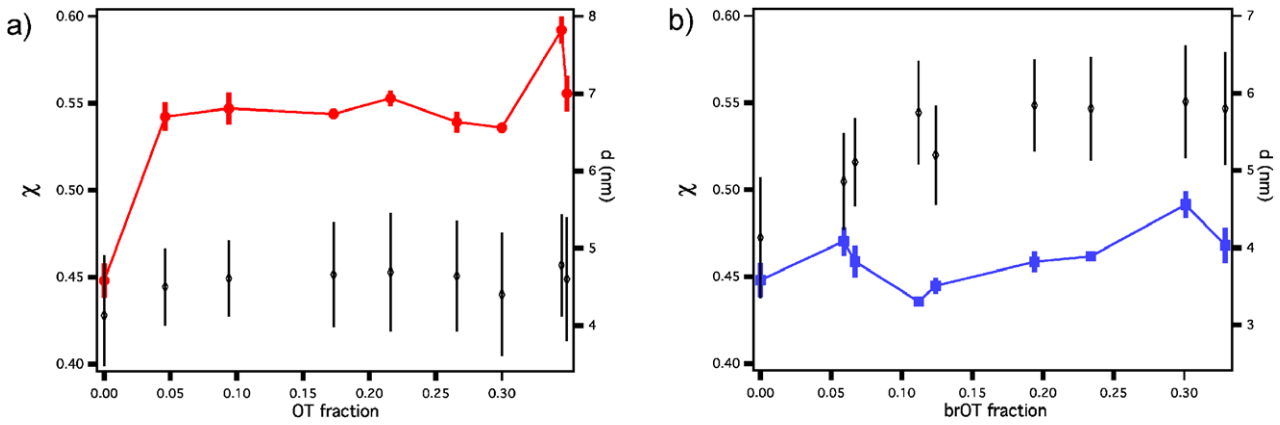

Figure 2. The χ values for the series MUA : OT (left, red) and MUA : brOT (right, blue) are plotted together with the diameter sizes of the initial nanoparticles used for the titration measured by TEM (χ: symbols with a solid line, TEM: black symbols). The error bars in the titration points correspond to the standard deviations for three independent titrations.

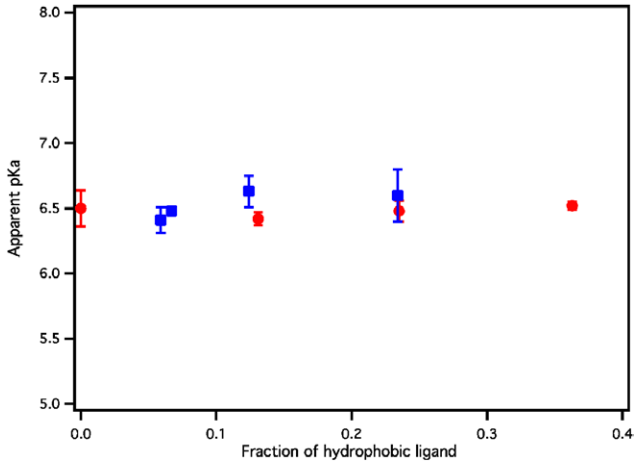

Figure 3. Apparent pKa values for gold nanoparticles covered by MUA and (br) OT ligands in different ratios (the MUA and MUA : OT series are shown as blue squares, and the MUA : brOT series as red circles).

performed with the MUA in the carboxylate state, it is necessary that the pH is several units above the pKa. For this reason, we have determined the apparent pKa of the MUA : OT and MUA : brOT nanoparticles using a modified protocol from the ones present in the literature (see supporting info, SI) [29, 30].

We find that the value of pKa for MUA nanoparticles with a diameter of 4–5 nm is equal to 6.3, which is consistent with the one reported in the literature by Wang *et al* (pKa = 6.5 for a diameter of 4.6 nm [29]) and much higher than the one of free MUA ligands (pKa ~ 5). When introducing OT or brOT ligands to the shell, we observed that the presence of these hydrophobic ligands with a percentage of up to almost 40% of the total ligands had no significative effect on the apparent pKa (figure 3). This value is quite below the experimental pH used in the titration experiment (~12) ensuring a totally deprotonated MUA.

The presence of hydrophobic ligands should in principle increase the spacing between the different ligands and hence the degree of ionization. This could produce a shift of the pKa to lower values in a similar way to the one observed by Wang *et al* with a decrease of pKa with an increase in the curvature of the nanoparticles (smaller sizes). The constant value of the apparent pKa that we observe in our results agrees more with the results observed by Charron *et al* where no significative change was observed with the change of nanoparticle curvature [30]. In our case the constant pKa could also be explained considering the length of the hydrophobic moiety and its structural arrangement on the surface of the nanoparticles. OT and brOT are shorter than MUA ligands and they lie below the charged headgroups. The presence of nanodomains, for the case of OT, of different sizes and shapes could also play an important role. These nanodomains dictate the amount of interfaces between charged and hydrophobic moieties. In our case these two contributions play a combined role in minimizing or canceling the contribution due to the presence of the hydrophobic moiety.

4. Conclusions

We have reported new results that show the influence of hydrophobic moiety and nanostructuring on the stability of charged nanoparticles by a co-precipitation experiment using oppositely charged nanoparticles. We studied a series of negatively charged nanoparticles containing an increasing amount of hydrophobic ligands by titrating them with oppositely (positively) charged nanoparticles. When hydrophobic ligands that tend to form a random distribution are used, no significative effect is observed in the precipitation point expressed as the charge ratio. Nanoparticle size changes also don't play a role in shifting the co-precipitation point. For ligands that tend to form patches a huge increase of the precipitation parameter and dependence on nanoparticle size changes are observed. A comparison between the two series of nanoparticles suggests the role played by hydrophobic nanostructuring in the colloidal stability of charged nanoparticles.

The effect of changing the properties of stability of nanoparticles is similar to the one observed on the interfacial energies of patchy nanoparticles. We believe that this phenomenon can have strong implications in the design of colloidal systems with the desired solvation properties and stability in solution. However more experiments are needed to fully elucidate the

influence of nanostructuring on the interfacial properties of nanoparticles.

Acknowledgments

We would like to acknowledge the help of Yannick Baumgartner and Marie-Claude Bay with the pKa measurements, and the financial support of the Swiss National Foundation.

References

[1] Dickinson E 2015 Colloids in food: ingredients, structure, and stability *Annu. Rev. Food. Sci. Technol.* **6** 211–33
[2] Talapin D V, Lee J S, Kovalenko M V and Shevchenko E V 2010 Prospects of colloidal nanocrystals for electronic and optoelectronic applications *Chem. Rev.* **110** 389–458
[3] Kim S H, Lee S Y, Yang S M and Yi G R 2011 Self-assembled colloidal structures for photonics *NPG Asia Mater.* **3** 25–33
[4] Matijevic E 2008 *Medical Applications of Colloids* (New York: Springer)
[5] Howes P D, Chandrawati R and Stevens M M 2014 Colloidal nanoparticles as advanced biological sensors *Science* **346** 1247390
[6] Kralchevsky P, Miller R and Ravera F 2013 *Colloid and Interface Chemistry for Nanotechnology* (Boca Raton, FL: Taylor and Francis)
[7] Israelachvili J N 2011 *Intermolecular and Surface Forces* (Burlington, MA: Academic)
[8] Grasso D, Subramaniam K, Butkus M, Strevett K and Bergendahl J 2002 A review of non-DLVO interactions in environmental colloidal systems *Rev. Environ. Sci. Biotechnol.* **1** 17–38
[9] Kalsin A M, Kowalczyk B, Smoukov S K, Klajn R and Grzybowski B A 2006 Ionic-like behavior of oppositely charged nanoparticles *J. Am. Chem. Soc.* **128** 15046–7
[10] Kalsin A M, Fialkowski M, Paszewski M, Smoukov S K, Bishop K J M and Grzybowski B A 2006 Electrostatic self-assembly of binary nanoparticle crystals with a diamond-like lattice *Science* **312** 420–4
[11] Kalsin A M, Kowalczyk B, Wesson P, Paszewski M and Grzybowski B A 2007 Studying the thermodynamics of surface reactions on nanoparticles by electrostatic titrations *J. Am. Chem. Soc.* **129** 6664–5
[12] Bishop K J M, Kowalczyk B and Grzybowski B A 2009 Precipitation of oppositely charged nanoparticles by dilution and/or temperature increase *J. Phys. Chem.* B **113** 1413–7
[13] Bishop K J M, Chevalier N R and Grzybowski B A 2013 When and why like-sized, oppositely charged particles assemble into diamond-like crystals *J. Phys. Chem. Lett.* **4** 1507–11
[14] Umar A and Choi S M 2013 Aggregation behavior of oppositely charged gold nanorods in aqueous solution *J. Phys. Chem.* C **117** 11738–43
[15] Jackson A M, Myerson J W and Stellacci F 2004 Spontaneous assembly of subnanometre-ordered domains in the ligand shell of monolayer-protected nanoparticles *Nat. Mater.* **3** 330–6
[16] Jackson A M, Hu Y, Silva P J and Stellacci F 2006 From homoligand- to mixed-ligand-monolayer-protected metal nanoparticles: a scanning tunneling microscopy investigation *J. Am. Chem. Soc.* **128** 11135–49
[17] Ong Q K, Reguera J, Silva P J, Moglianetti M, Harkness K, Longobardi M, Mali K S, Renner C, De Feyter S and Stellacci F 2013 High-resolution scanning tunneling microscopy characterization of mixed monolayer protected gold nanoparticles *ACS Nano* **7** 8529–39
[18] Liu X, Yu M, Kim H, Mameli M and Stellacci F 2012 Determination of monolayer-protected gold nanoparticle ligand-shell morphology using NMR *Nat. Commun.* **3** 1182
[19] Harkness K M, Balinski A, McLean J A and Cliffel D E 2011 Nanoscale phase segregation of mixed thiolates on gold nanoparticles *Angew. Chem. Int. Ed. Engl.* **50** 10554–9
[20] Moglianetti M, Ong Q K, Reguera J, Harkness K, Mameli M, Radulescu A, Kohlbrecher J, Jud C, Svergun D and Stellacci F 2014 Scanning tunneling microscopy and small angle neutron scattering study of mixed monolayer protected gold nanoparticles in organic solvents *Chem. Sci.* **5** 1232–40
[21] Singh C, Ghorai P K, Horsch M A, Jackson A M, Larson R G, Stellacci F and Glotzer S C 2007 Entropy-mediated patterning of surfactant-coated nanoparticles and surfaces *Phys. Rev. Lett.* **99** 226106
[22] Verma A, Uzun O, Hu Y H, Hu Y, Han H S, Watson N, Chen S L, Irvine D J and Stellacci F 2008 Surface-structure-regulated cell-membrane penetration by monolayer-protected nanoparticles *Nat. Mater.* **7** 588–95
[23] Kuna J J, Voitchovsky K, Singh C, Jiang H, Mwenifumbo S, Ghorai P K, Stevens M M, Glotzer S C and Stellacci F 2009 The effect of nanometre-scale structure on interfacial energy *Nat. Mater.* **8** 837–42
[24] Chandler D 2005 Interfaces and the driving force of hydrophobic assembly *Nature* **437** 640–7
[25] Kim H, Carney R P, Reguera J, Ong Q K, Liu X and Stellacci F 2012 Synthesis and characterization of Janus gold nanoparticles *Adv. Mater.* **24** 3857–63
[26] Zheng N, Fan J and Stucky G D 2006 One-step one-phase synthesis of monodisperse noble-metallic nanoparticles and their colloidal crystals *J. Am. Chem. Soc.* **128** 6550–1
[27] Reguera J, Ponomarev E, Geue T, Stellacci F, Bresme F and Moglianetti M 2015 Contact angle and adsorption energies of nanoparticles at the air-liquid interface determined by neutron reflectivity and molecular dynamics *Nanoscale* **7** 5665–73
[28] Schneider C A, Rasband W S and Eliceiri K W 2012 NIH Image to ImageJ: 25 years of image analysis *Nat. Methods* **9** 671–5
[29] Wang D, Nap R J, Lagzi I, Kowalczyk B, Han S, Grzybowski B A and Szleifer I 2011 How and why nanoparticle's curvature regulates the apparent pKa of the coating ligands *J. Am. Chem. Soc.* **133** 2192–7
[30] Charron G, Huhn D, Perrier A, Cordier L, Pickett C J, Nann T and Parak W J 2012 On the use of pH titration to quantitatively characterize colloidal nanoparticles *Langmuir* **28** 15141–9
[31] Kowalczyk B, Kalsin A M, Orlik R, Bishop K J, Patashinskii A Z, Mitus A and Grzybowski B A 2009 Size selection during crystallization of oppositely charged nanoparticles *Chemistry* **15** 2032–5